RADIO-ECHO OBSERVATIONS OF METEORS IN THE ANTARCTIC

By C. S. Nilsson* and A. A. Weiss†

[*Manuscript received May 24, 1961*]

Summary

Radio observations of meteors have been made at Mawson on the Antarctic continent since 1957, with a coherent pulse radar equipment operated at a frequency of 34 Mc/s. Heights and directions of reflection points are available for about 10% of the echoes, and temporal variations in these characteristics, together with the diurnal variations in the total echo rate, are analysed and discussed. All the variations observed in these characteristics agree with predictions based on a three-source model for the distribution of the radiants of sporadic meteors. This model distribution, which is symmetrical about the ecliptic, consists of a broad apex source and more concentrated sources near the Sun and antisun. The integrated intensities of the three sources are found to be approximately equal. There is evidence that the meteor echo rate is depressed at times of radio black-out, and it is suggested that periods of exceptionally high meteor activity observed during the summer months could be caused by abnormal ionospheric conditions.

I. Introduction

Radio observations of meteors have been made at Mawson (68 °S., 67 °E.) on the Antarctic coast since 1957. The equipment used is a coherent pulse radar with the following characteristics :

p.r.f. $=750$ c/s	f $=34$ Mc/s
pulse length $=15$ μs	peak pulse power $=5$ kW.

The antennas are $\frac{1}{2}\lambda$ dipoles $\frac{1}{4}\lambda$ above an earth mesh, and supported near the ends by vertical piping. A double pulse discriminator system is used to improve the signal/noise ratio, but the local noise level is so high that the maximum usable receiver sensitivity gives a limiting power at the receiver of $\bar{\omega}=4\times10^{-12}$ W. This is equivalent to a limiting line density of $\alpha_0=3\times10^{11}$ electrons/cm.

The equipment is basically designed to measure winds in the meteor region by comparing, at various spaced antennas, the phases of the signal returned from a meteor trail (Robertson, Liddy, and Elford 1953). Thus the direction cosines and heights of the reflection points are known for about 10% of the echoes. As has already been shown (Weiss 1957, 1959), analysis of these characteristics of the reflection points provides information on the distribution of meteor radiants.

This paper presents the results of astronomical interest so far obtained from the Mawson recordings, with particular emphasis on the distribution of the radiants of sporadic meteors. The basic data are the characteristics of reflection

* Department of Physics, University of Adelaide.

† Division of Radiophysics, C.S.I.R.O., University Grounds, Chippendale, N.S.W.

points just mentioned, and the temporal variations in the total rate of echoes detected by the equipment. In interpreting these data we adopt the now well-established distribution of sporadic radiants based on three sources, all of which lie on the ecliptic, namely, a broad apex source and more concentrated sources near the Sun and antisun. Our results suggest that the integrated intensities of all three sources are approximately equal.

The symbols used in this paper are defined in the Appendix. All times quoted throughout this paper are in Local Time (L.T. = U.T. + 4 hr).

TABLE 1

SUMMARY OF HEIGHT DATA ANALYSED

Month	Number of Meteors	Mean Height (km)	r.m.s. Deviation (km)
Oct.–Nov. 1957 ..	135	95·2	13·1
Dec. 1957 ..	296	96·0	10·4
Jan. 1958 ..	145	92·8	10·1
Feb. 1958 ..	118	91·2	9·4
Mar.–Apr. 1958 ..	81	91·7	12·0
Dec. 1958 ..	342	95·4	10·0
Jan. 1959 ..	317	95·3	9·6

II. AZIMUTHAL DISTRIBUTION OF REFLECTION POINTS

We shall first ascertain the information on the source distribution of the radiants of sporadic meteors which is contained in the azimuth data. Weiss (1957) has shown that this can be achieved through use of the property of specular

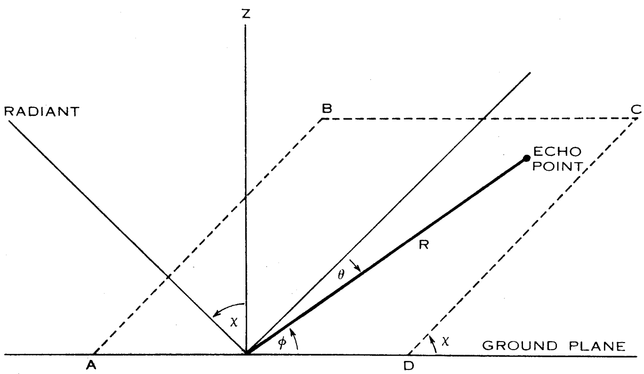

Fig. 1.—The geometry of echo detection. The echo plane *ABCD* is normal to the radiant direction. $\frac{1}{2}\pi-\theta$ is the direction of the echo, at slant range *R*, in the echo plane measured from the horizontal, and φ is the elevation of the echoing point.

reflection of the meteor trail. The reflection points for trails proceeding from a given radiant of zenith angle χ must all lie in a plane perpendicular to the observer-radiant line and have an elevation less than or equal to χ. Since the antennas have maximum gain vertically overhead, it follows that the most likely azimuth for the reflection points is 180° removed from that of the radiant. This corresponds to $\theta = 0$ in Figure 1.

The echoes analysed (see Table 1) were recorded during the summers of 1957/58 and 1958/59. Figure 2 shows the azimuthal distribution of reflection

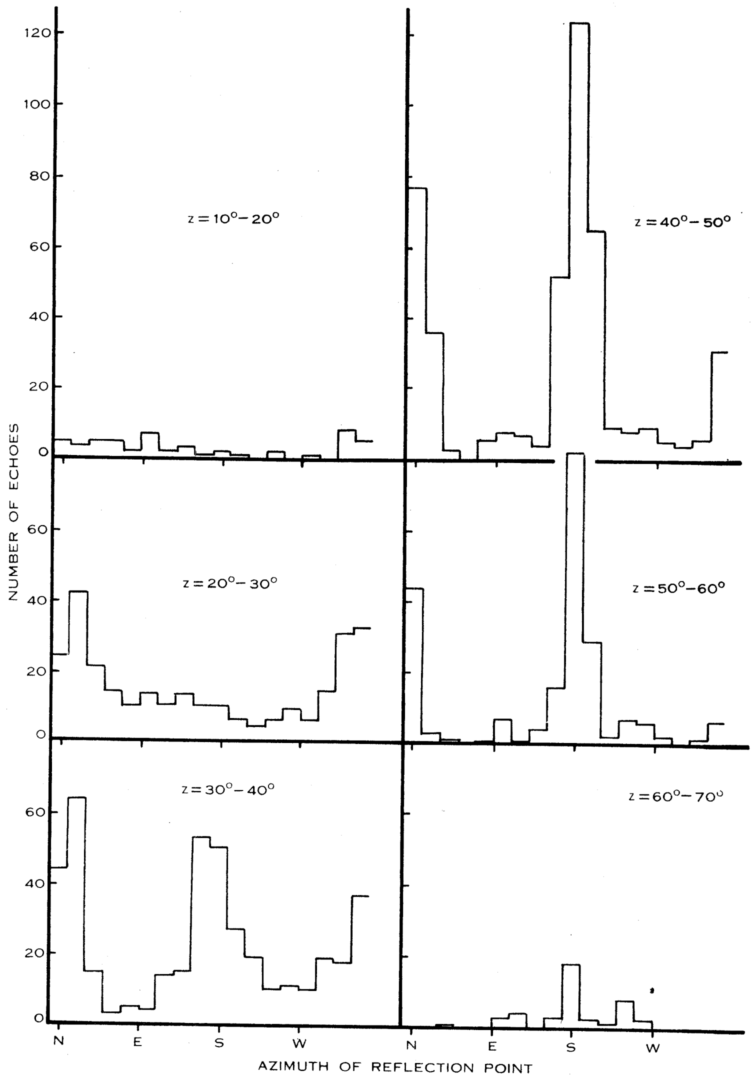

Fig. 2.—The observed azimuthal distributions of reflection points for 10° intervals of zenith angle.

points for 10° intervals of zenith angle. The obvious preference for reflection points to lie in the north or south can be explained by the form of the antenna polar diagram. The end supports of the dipoles are conducting waterpipe and presumably give the antennas loop characteristics. The dipoles are aligned on the east-west line, hence we have in effect a broad figure-of-eight beam to the north and south.

Figure 3 shows the diurnal variation of the numbers of echoes in each of the four azimuthal groups centred on north, south, east, and west. The diurnal variation of the total number of echoes of quality sufficient to give reflection point direction cosines is given in Figure 3 (*e*). This variation, which applies to only 10% of the total echoes detected, is not the same as the overall diurnal variation for December–January given in Section V, a fact undoubtedly due to the selection processes involved in choosing echoes for detailed analysis, as opposed to the requirements for the recognition of echoes.

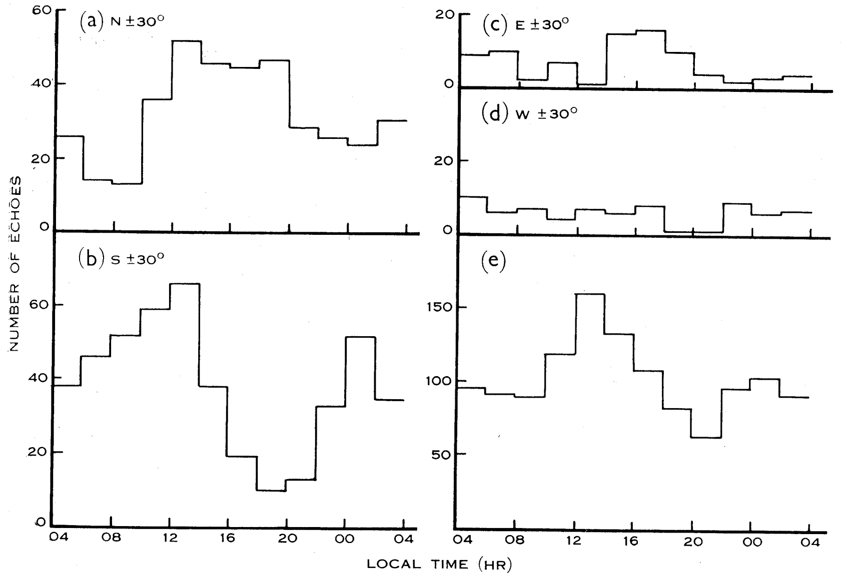

Fig. 3.—The diurnal variations of the numbers of echoes. (*a*)–(*d*) In different azimuth groups, (*e*) the diurnal variation of all echoes without regard to azimuth.

We will now show that these diurnal variations in azimuth distribution can be explained by assuming a distribution of sporadic radiants based on three sources, namely, a broad apex source and more concentrated sources near the Sun and antisun. All three are taken to lie on the ecliptic, the latter two having ecliptic longitudes 70° removed from the apex. This source model is based on the radio results of Hawkins (1956) and of Weiss (1960*b*), and the visual results of Hawkins and Prentice (1957).

There is a peak in Figure 3 (*c*) between 14 and 19 hr which can possibly be attributed to the Sun source at low elevation (about 20°) in the west, but the antenna polar diagram is too uncertain to permit a useful discussion of the east-west results.

The ratio of the numbers of northern to southern reflection points is more useful. Figure 4 is a logarithmic plot of the north/south ratio obtained from the data presented in Figure 3. Upper and lower transit times of the three sources are shown, with the exception of the lower transit of the antisun source, which does not contribute to the echo rate at lower transit during the summer months. At apex lower transit in January the apex source is centred on zenith angle $Z=104°$ in the south, and from the arguments advanced in the first paragraph of this section we can expect a concentration of echoing points in the north at this time (18 hr). The observations (see Fig. 4) conform to this expectation. The upper transit of the apex at 06 hr should be marked by a concentration of reflection

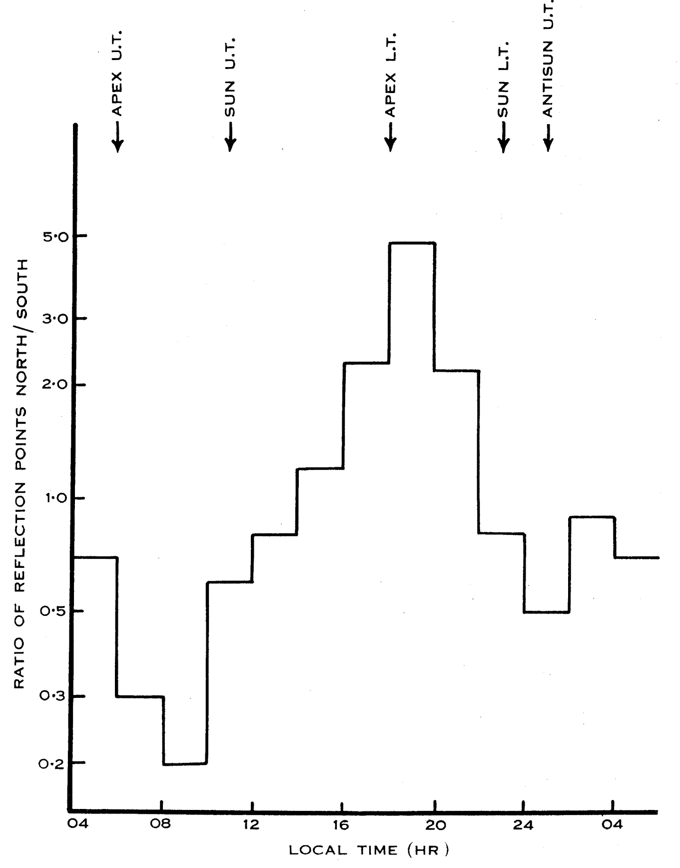

Fig. 4.—The diurnal variation of the ratio of northern to southern reflection points. The transit times of the various sources are indicated near the top of the diagram (U.T.=upper transit, L.T.=lower transit).

points in the south, which should appear as a minimum in Figure 4. Actually, the minimum is seen to fall midway between the upper transit of the apex and the upper transit of the Sun source at 11 hr. Since the strengths of the Sun and antisun sources are approximately equal, this result implies that these sources are stronger than indicated by the visual results of Hawkins and Prentice (which applied only to the antisun source). This conclusion as to the relative strengths of the sources is substantiated by the observed diurnal rate variations analysed later in Section V.

The antisun source does not rise far above the horizon in January, but at upper transit near 01 hr should give echoes in the south. However, the lower transit of the Sun source near 23 hr should give about the same number of echoes in the north. The step near 00 hr in Figure 4 is not inconsistent with contributions from these two sources.

III. Zenith Angle Distribution of Reflection Points

Figure 5 (*a*) shows the distribution in zenith angle of the reflection points of all echoes, without regard to azimuth. This distribution has a broad maximum between zenith angles 30 and 50°, and there are very few reflection points with zenith angles exceeding 50°. These observed features may be compared with the result of Kaiser (1953), who showed that for a $\frac{1}{2}\lambda$ dipole $\frac{1}{4}\lambda$ above ground, and a uniform radiant distribution, the peak of the zenith angle distribution is fairly sharp and occurs at $z=50°$. The differences between our observed distribution and the theoretical one can be fully accounted for by the departure of the assumed

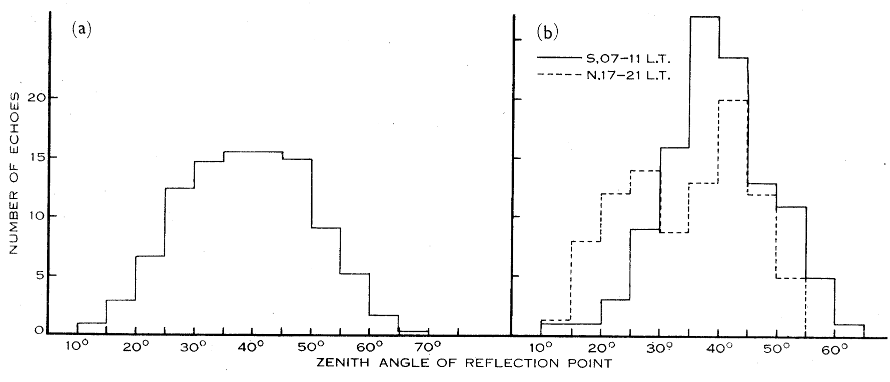

Fig. 5.—The zenith angle distribution of (*a*) all echoes without regard to time or azimuth; (*b*) of two groups of echoes : —— those with southern reflection points received between 07 and 11 hr, --- those with northern reflection points received between 17 and 21 hr.

radiant distribution from uniformity ; in fact, our assumed radiant distribution implies that the elevation of any of the source centres never exceeds 45°. The lack of reflection points with zenith angles exceeding 50° is consistent with this source distribution and the geometry of specular reflection. There is thus no evidence that the distortion of the antenna polar diagram, inferred from the azimuth distributions, extends to the variation of the antenna gain with zenith angle.

With this assurance, we now proceed to examine the zenith angle distribution of selected groups of echoes for agreement with predictions based on our assumed source function.

The northern echoes detected between 17 and 21 hr have been associated with the apex source at lower transit, and the southern echoes detected between 07 and 11 hr with the apex and Sun sources at upper transit. As a group, the reflection points of the former echoes should have smaller zenith angles than the latter. The zenith angle distributions for the appropriate groups of echoes, plotted in Figure 5 (*b*), indicate that this is the case ; the mean zenith angle for northern echoes is 40°, for southern echoes 45°.

Further confirmation that the sources in the south (which produce echoes in the north) are lower in the sky than the sources in the north (which produce echoes in the south) is afforded by a detailed examination of Figure 2. We observe that (*a*) there is no peak in the south for z less than 30°, and (*b*) no peak in the north for z greater than 60°. From Figure 1, the zenith angle of the reflection point, z, is greater than or equal to the elevation of the radiant, $90\text{-}\chi$. From (*a*) we infer that there are not many radiants in the north for which $\chi > 60°$. This argument is only strictly true for a point radiant, but in fact can be extended to a source of radiants with maximum density in the centre. There is thus no source in the north for which $Z > 60°$, i.e. no source of low elevation. Again, from the argument of Section II, paragraph 1, we use the most probable relation, $90 - Z = z$, and infer from (*b*) that there is no source in the south for which $Z < 30°$, i.e. no source of high elevation. For $30 < z < 60$, there are peaks both in the north and south, indicating both southern and northern sources of reasonable elevation.

We thus conclude that both azimuth and zenith angle data are consistent with our assumed source distribution. It is possible to go a little further, and to use the data of Figure 2 to obtain an estimate of the diameter of the apex source. Between $z = 50$ and 60° there is still a pronounced peak in the north. If we assume that this is due to the lower transit of the apex source, for which $Z = 104°$ in January, the source must extend for at least $104° - (90° - 55°) = 70°$ approximately from the centre. According to the apex source density distribution function derived from the radio results of Weiss and illustrated in Figure 14, the source density is reduced by a factor of only from 2 to 3 at 70° from the centre.

IV. Height Distribution

The heights of the echoing points of the sporadic meteors whose azimuths and zenith angles have been discussed in the preceding sections have also been measured. Heights were determined from zenith angles and slant ranges. The error in the slant range is of the order of 1%, but the errors in the heights are determined largely by the errors in the azimuth measurements. These are rather difficult to assess, but we estimate an error of ± 5 km in the individual heights.

The mean height, and the r.m.s. deviation from the mean, of the height distributions for each month separately are listed in Table 1. There is no evidence that the low mean heights found for January–April 1958 result from errors in equipment calibration, and data for all months have been combined on the assumption that the variations in mean height from month to month are real. There is no apparent seasonal variation in the mean height, in agreement with measurements made at Adelaide over a more extended period with similar equipment (Weiss 1959), but the possibility of a seasonal variation in the r.m.s. deviation, with a minimum in February, cannot be dismissed.

The overall height distribution for all Mawson echoes is sketched in Figure 6 (*a*), where it is compared with the height distribution measured at Adelaide (Weiss 1959). Both distributions have been normalized to equal areas under the histograms. The higher mean height at Mawson is probably a latitude effect. At Mawson the minimum zenith angles of the sources of sporadic meteors are some 30° greater than at Adelaide, and a simple calculation shows that this is quite adequate to explain the difference of 2 km or so in the mean heights recorded at the two stations. The long tails of the Mawson height distribution, which are responsible for the high value of the r.m.s. deviation, are real, as will be shown presently. Similar tails are not present in the Adelaide distribution, but it is thought that this is a consequence of selection of echoes for analysis rather than an indication of their absence from the Adelaide recordings.

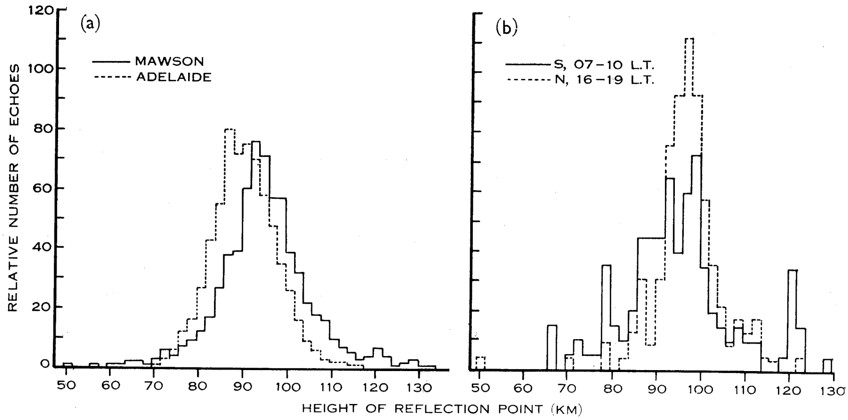

Fig. 6 (*a*).—The height distribution of reflection points for Adelaide and Mawson.
Fig. 6 (*b*).—The height distribution of two groups of echoes : —— those with southern reflection points received between 07 and 10 hr ; - - - those with northern reflection points received between 16 and 19 hr.

The diurnal variations in the mean height and the r.m.s. deviation from the mean have been ascertained for each month separately. There are no strong variations from month to month and the data have been pooled. The average diurnal variation in each parameter over the summer months is illustrated in Figure 7.

As already found from the Adelaide measurements, the diurnal variation in the mean height is small. Maximum height occurs at 17 hr when the apex is near lower transit ; this is the only indication that the mean height is influenced to any extent by the position in the sky of the sources of sporadic meteors.

On the other hand, the diurnal variation in the r.m.s. deviation is large, and its reality is made more plausible by the excellent agreement between its phase and the phases of the azimuthal diurnal variations presented in Figure 4. The r.m.s. deviation of the height distribution is largest at a time midway between the upper transits of the apex and Sun sources, and smallest near the lower transit of the apex source. Further information on the nature of the diurnal variation in width of the height distribution is contained in Figure 6 (*b*), in which we have drawn height distributions for two selected groups of meteors. These two groups dominate the total echo rate and so largely determine the properties of the height distribution, at the respective times. The first group, comprising all meteors detected between 07–10 hr with echoing points located to the south, presumably originates from the combined Sun and apex sources near upper transit. The second group, which includes all meteors detected from 16–19 hr with echoing points to the north, proceeds from the apex source near lower transit. It will be seen that the latter distribution is much narrower than,

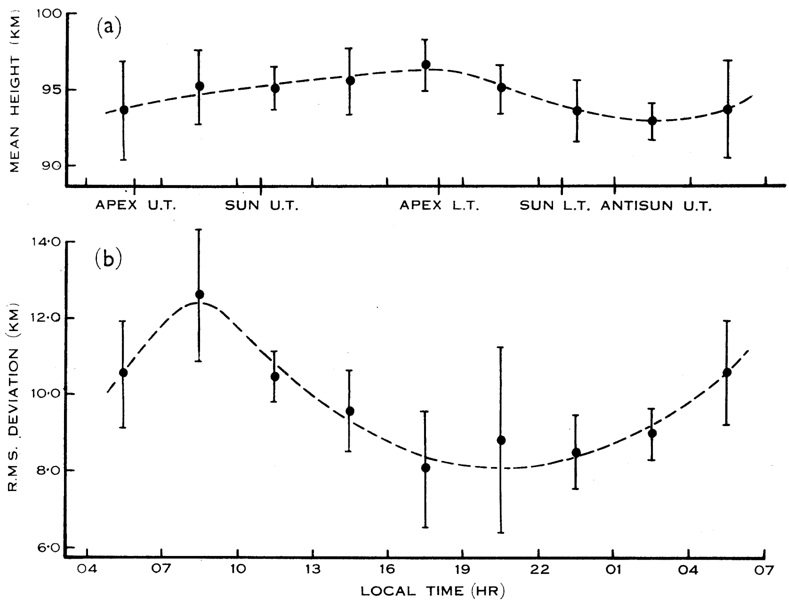

Fig. 7 (*a*).—The diurnal variation of the mean height for the summer months. Fig. 7 (*b*).—The diurnal variation of the r.m.s. deviation from the mean height. The vertical lines represent the r.m.s. deviations of mean values which are indicated by dots. The transit times of the various sources are indicated (U.T. = upper transit, L.T. = lower transit).

and lacks the long initial tail of, the former. From the times of occurrence of the maximum and minimum of Figure 7 (*b*), in relation to the times of upper and lower transit of the apex and Sun sources, it is clear that the Sun source can make little contribution to the narrow height distribution found for the apex source at lower transit, whereas it does contribute strongly to the wider distribution found at 07–10 hr. The inference is that trails of Sun source meteors are formed lower in the atmosphere than apex source meteors. Since the heights of formation of trails of meteors which differ only in velocity v depend on $\ln v$, this suggests that Sun source meteors possess lower speeds than apex source meteors. The occurrence of maximum mean height at apex lower transit could then be due simply to the low relative number of detectable Sun source meteors at that time, but the large zenith angle of the apex source may also be a contributing factor.

Incidentally, the absence of the long tail of low heights at apex lower transit suggests that the tails in the overall Mawson distribution (Fig. 6 (*a*)) are real.

V. The Diurnal Rate Variation

In this section we discuss the calculation of the theoretical diurnal variation in the echo rate and compare it with the observed results.

A table of α_0, the line density of a barely detectable echo, can be prepared as a function of the zenith angle and azimuth of the reflection point from the formulae for Lovell-Clegg and persistent scattering given in the Appendix. The table, which is not reproduced, predicts a cut-off of echoes at zenith angles larger than 65°, where $\alpha_0 \simeq 10^{14}$ electrons/cm. This corresponds to a maximum range of detectable echoes of 250 km, and this was observed in practice. Also, Figure 5 (*a*) shows a cut-off around $z=65°$, and we conclude that the sensitivity figures used are reasonable.

To use this table of α_0-values for a determination of the sporadic diurnal rate variation, we first assume independence of the antenna polar diagram on azimuth, an assumption which is modified at the end of the calculations.

The first step is to calculate the response of the equipment, $f(\chi)$, to a point radiant at zenith angle χ. Kaiser (1953) has given a formula for the echo rate, which is equivalent to

$$f(\chi)=\cos \chi \int_{\theta=0}^{\frac{1}{2}\pi} \frac{R\mathrm{d}\theta}{R/R_E+\sin \varphi} \cdot \frac{1}{\alpha(\theta)}, \tag{1}$$

where the mass distribution parameter s is assumed to have the value $s=2$ for sporadics. Here R_E is the radius of the Earth, φ is the elevation of the echo, and θ is as shown in Figure 1. Because of the cut-off in echo rate at $z=65°$, $R/R_E \ll \sin \varphi$ and it is adequate to use flat earth geometry for which $h=R \sin \varphi$. Also $\sin \varphi=\sin \chi \cos \theta$. Introducing a mean height, $\bar{h}$, for reflection points, (1) may be written

$$f(\chi)=\frac{\bar{h} \cos \chi}{\sin^2 \chi} \int_{\theta=0}^{\frac{1}{2}\pi} \frac{\mathrm{d}\theta}{\alpha(\theta) \cdot \cos^2 \theta}, \tag{2}$$

from which $f(\chi)$ may be found, making use of the table of α_0 already prepared. $f(\chi)$ for the Mawson equipment is illustrated in Figure 8 (*a*).

The next step, the calculation of the echo rate as a function of the zenith angle of the source, is quite general and applicable to any function $f(\chi)$ and to any extended source whose density is a function only of the elongation from the centre of the source. It is described in the Appendix, together with the details of the apex, Sun, and antisun source distributions.

For any one of the sources, therefore, we have now established the variation of the echo rate as a function of the zenith angle of the source. This variation $F(z)$ for the Mawson equipment is shown in Figure 8 (*b*), where the contributions from each source have been normalized to give the same peak rate within the range of the zenith angles of the sources expected at Mawson. This corresponds to the maximum density of the Sun and antisun sources being 4·5 times that of the apex source. The visual results of Hawkins and Prentice indicated a ratio of only 1·5, but the Mawson diurnal sporadic rate variation best fits the theoretical predictions if a larger ratio is used. This is discussed more fully later in this section.

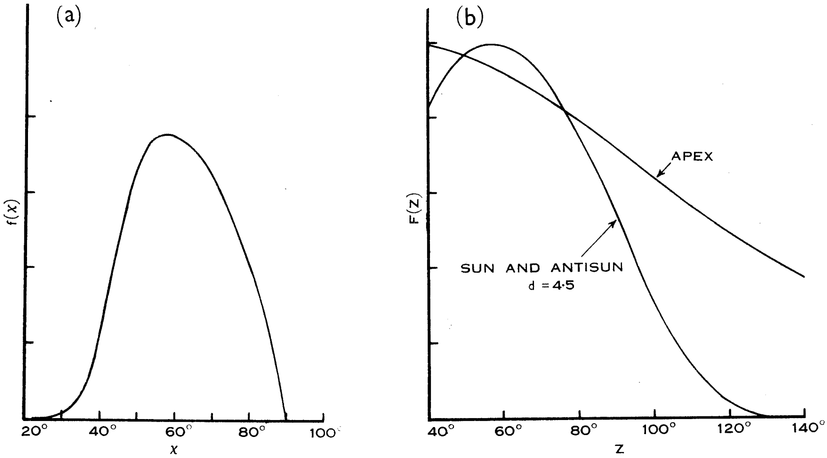

Fig. 8 (*a*).—The equipment response function, $f(\chi)$ (see Section V) plotted against the zenith angle χ of a radiant.

Fig. 8 (*b*).—The rate variation function, $F(Z)$ (see Appendix) plotted against the zenith angle Z of the three sources. d is the ratio of the peak source density of the Sun and antisun sources to that of the apex source.

It remains to allow for the azimuth variation of the aerial polar diagram. The assumption that the azimuth of the radiant is 180° removed from that of the reflection point is valid *only on the average* for either a point radiant or an extended source of radiants. With this limitation in mind, we can weight the source distribution as a function of azimuth of the source, although in reality all we should weight are the reflection points. The weighting function is based on the data from Figure 2 and is set out in Table 2.

Table 2

AZIMUTH WEIGHTING FUNCTION

Hour Angle of Source . .	0– 2 12–14	3– 4 15–16	5– 7 17–19	8– 9 20–21	10–12 22–24
Weight	1	$\frac{1}{2}$	$\frac{1}{4}$	$\frac{1}{2}$	1

The only means of verifying this procedure was afforded by the δ-Aquarid shower of July–August. Figure 9 shows that the theoretical temporal variation in echo rate, based on the known movement of the radiant, fits the observations more closely when the dependence of the antenna polar diagram on azimuth is taken into account in this way.

Finally, we calculate the zenith angles of the three sources as a function of time, substitute for the zenith angle the appropriate echo rate from Figure 8 (*b*), weight this with the azimuth function, and add together the rates for all three sources. This has been done for each month separately and the resulting theoretical echo rates are shown in Figure 10.

Apex upper transit occurs at 06 hr, lower transit at 18 hr. The use of the azimuth weighting function and a Sun source to apex source peak density ratio as low as 1·5 results in a noticeable peak at 18 hr in the predicted echo rate, due to the apex source at lower transit. This is illustrated in Figure 10 for October and the summer months of December and January. There is no sign of such a peak in any of the observations for any months (see Fig. 11), so we conclude that

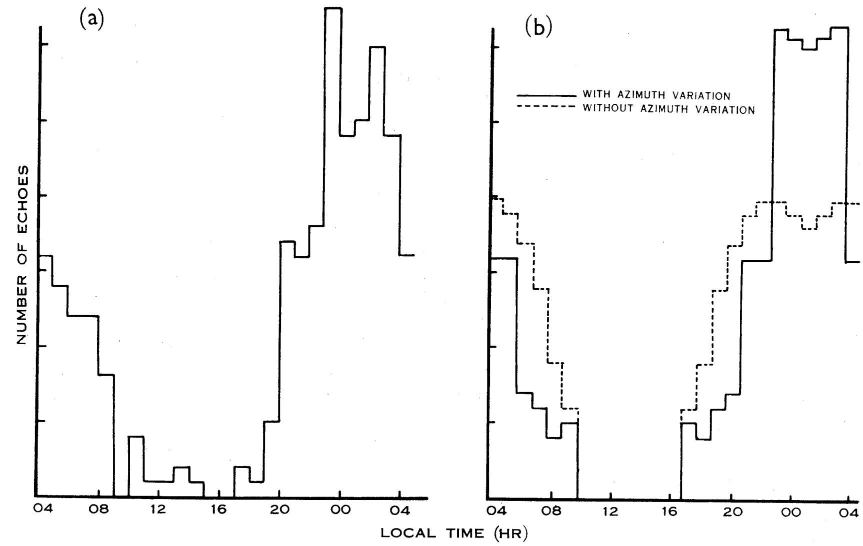

Fig. 9.—The temporal variation in the echo rate for the δ-Aquarid shower of July–August, 1957. (*a*) Observed, normalized to a mean rate of 11 echoes/hr. (*b*) Theoretical, plotted with and without allowance for the azimuth variation in the antenna polar diagram. The theoretical rates have been normalized to the same mean rate as the observations.

the Sun and antisun components are large enough to mask the effect. We have therefore used a peak density ratio of 4·5 in calculating the theoretical rates. This implies that the integrated contributions from the three sources are approximately equal, as the lower peak apex density is compensated by the greater extent of this source. Meek and James (1959), in the predictions for their forward-scatter experiments, used a three-point radiant model, weighting each radiant equally. This is approximately equivalent to assuming the integrated response from each source to have the same maximum value, as we have done in normalizing Figure 8 (*b*).

During the summer, when the azimuth and height data require a strong Sun source, the observed diurnal echo rate is high (even to the extent of showing a second peak, as in December 1958 and January 1959) from apex upper transit at 06 hr to Sun source upper transit at 11 hr. Choosing a value of peak density ratio of 4·5 leads to broader maxima in the theoretical rate curves than does a smaller value. These broad maxima are thus supported by the observations, which are shown in Figure 11.

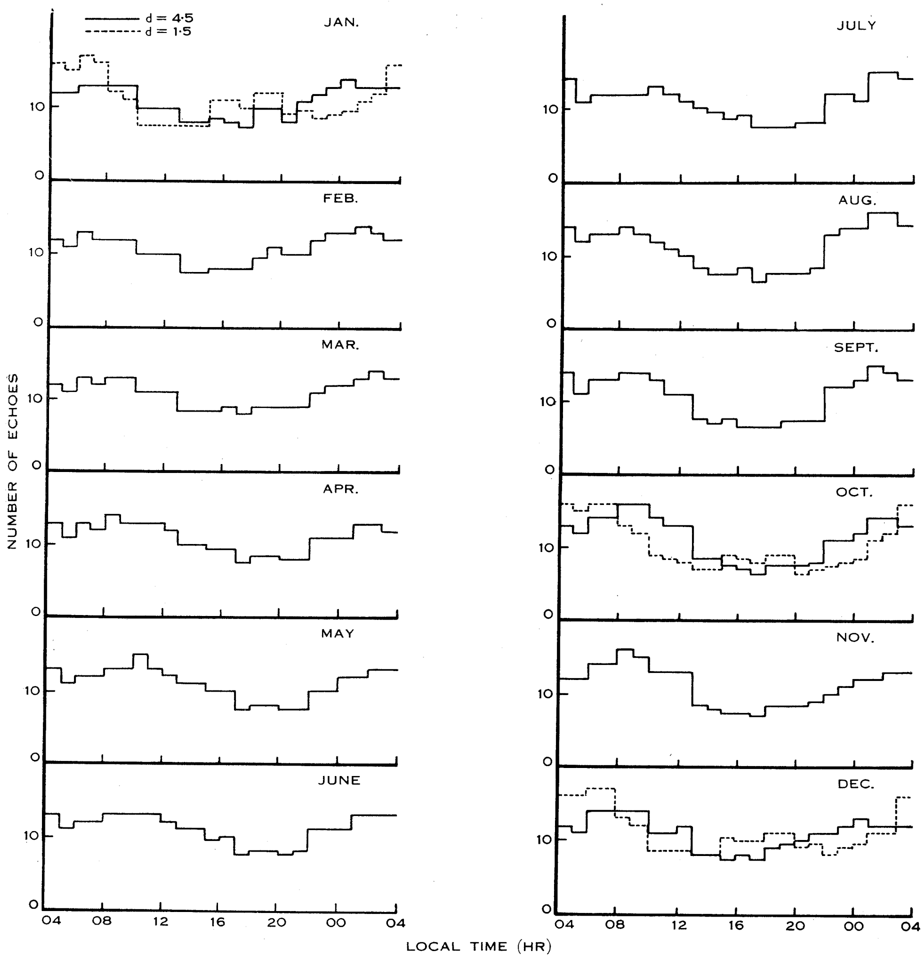

Fig. 10.—The theoretical diurnal rate variations of sporadic meteors at Mawson based on a distributed three-source model. *d* is the ratio of the peak source density of the Sun and antisun sources to that of the apex source. The echo rates have all been normalized to a mean rate of 11 echoes/hr.

The observed rates have been normalized to a mean echo rate of 11 per hour. The data have also been corrected as far as possible for equipment-off periods, but the high noise level introduces some uncertainty. This should not change the form of the diurnal variation, but it does necessitate the equipment operating at a rate as low as 2–3 echoes per hour for some periods. This leads to considerable scatter in the records. November 1957 and all 1960 rates are in this category.

Close examination shows that, while the general features of the observed and predicted rates are in agreement, there are certain dissimilarities. Between July and December the predicted minimum shifts from 19 hr to 16 hr, whereas the observed rates show the reverse effect, the minimum shifting from 17 hr in August to 20 hr in December. It is shown in Section VI, however, that ionospheric conditions appear to affect the echo rate, and this disagreement could

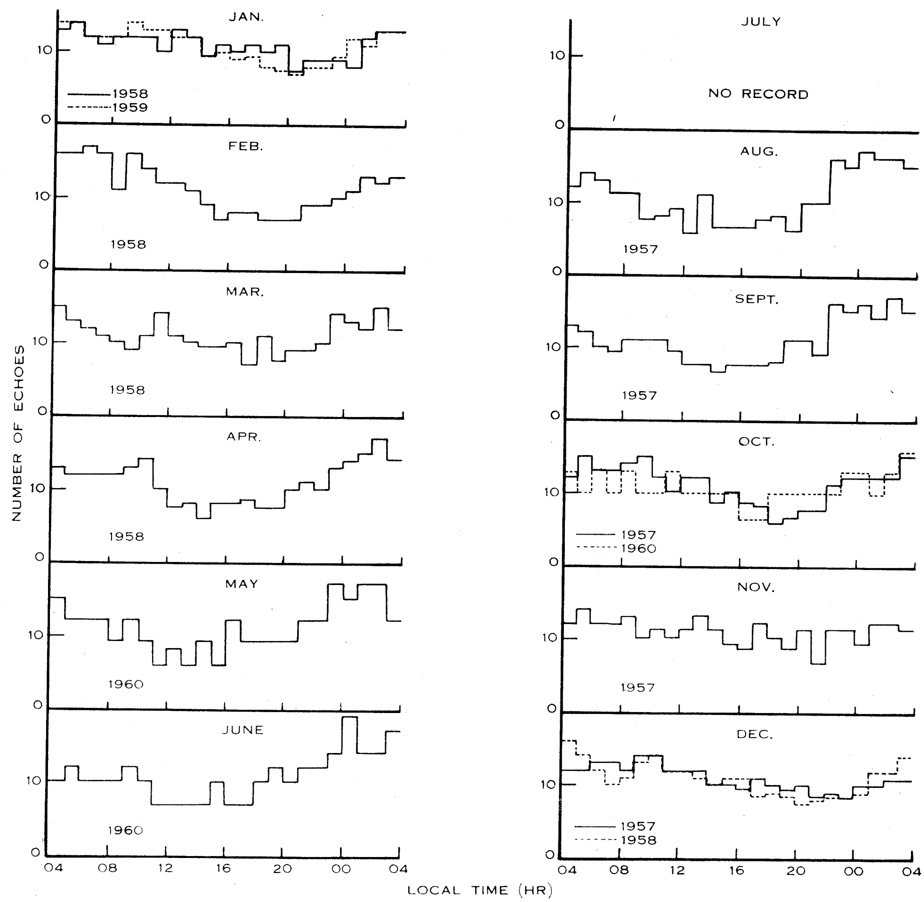

Fig. 11.—The observed diurnal rate variations of sporadic meteors, normalized to a mean rate of 11 echoes/hr.

well be due to some diurnal ionospheric effect, rather than an actual difference between our model and the true distribution of sporadic meteors. In view of the uncertainties in both the observed rate due to the high noise level at Mawson, and the predicted rate due to the variation in response with azimuth, the significance of minor features should not be overstressed.

The major features of the diurnal variation have repeated from year to year. Several repetitions are shown in Figure 11 for comparison.

Echo rates for July have been omitted because of the difficulty in separating the sporadic background from the δ-Aquarid shower activity. Both sets of activity have maxima occurring between 00 and 04 hr.

VI. The Daily and Seasonal Variation in Echo Rate

Because of unusually large variations in equipment sensitivity, introduced by severe operating conditions and large fluctuations in noise level, the seasonal variation in the total daily echo rate could not be determined. However, the variation in daily total echo rate, after smoothing out gross equipment changes and any possible seasonal variation, is plotted in Figure 12. The data have been smoothed by plotting in running groups of three.

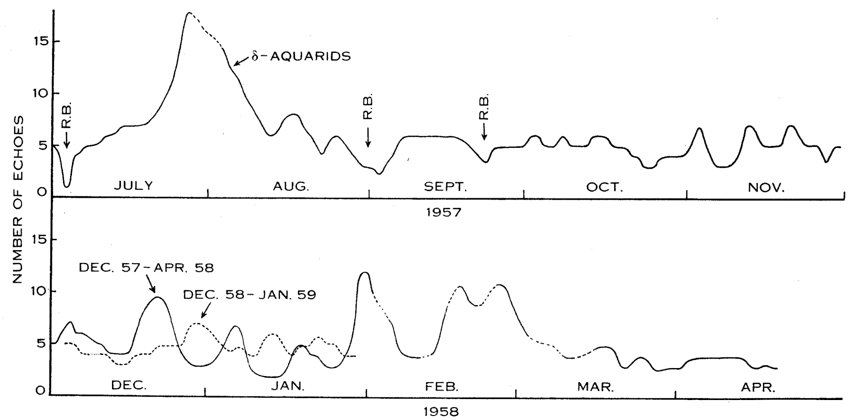

Fig. 12.—The fluctuations in daily echo rate, after correction for equipment and possible seasonal changes in the echo rate. R.B.=radio communication black-out.

The δ-Aquarid shower is the only major shower expected to be detected; it is prominent in July–August. There is also marked correlation between short periods of low rate and poor radio communications between Mawson and the rest of the world, known as "radio black-outs".* (Our records of radio black-outs at Mawson do not extend beyond September 1957.) The summer of 1957–58 has large variations in total daily rate. The increases from December 15 to December 24, January 26 to February 6, and February 12 to February 28 are probably significant. These increases do not show any shower characteristics, nor have they any tendency to repeat from year to year, as the months of December 1958 and January 1959 show. Any attempt to separate a presumed base level of sporadic activity from these periods of high count leaves a residual diurnal rate variation similar to the predicted and observed sporadic rate; the periods of low activity on either side of the high activity periods in question have been taken to represent the true observed sporadic rate for this test. Our conclusion is that these are real increases in the sporadic background rate. They

* McNamara (1961) has given a similar example of a marked decrease in the meteor echo rate during 12/13 November 1960, which he attributed to low-level absorption during a PCA event.

could be due either to true increases in the influx of meteors or to increases in the detection rate due to changes in the ionosphere. The latter hypothesis is supported by the absence of any abnormal activity in echo counts made at Adelaide with the high resolution radiant equipment (Weiss 1960*a*) over this period. The radio black-out periods indicate that ionospheric changes can inhibit the rate and it is conceivable that other changes could increase it. This possibility is enhanced by the fact that Mawson is located in the belt of maximum auroral frequency.

VII. Conclusions

Experience with the interpretation of the Mawson records has confirmed the opinion, reached in the analysis of records obtained with Adelaide equipments, that broad-beam antenna systems are not the most suitable for measuring the distribution of meteor radiants over the sky. Extraction of data from the Mawson records was hampered by the unfortunate azimuth variation in the antenna polar diagram, which basically arose from the necessity for mechanical stability of the antennas in the inclement environment of the Antarctic continent, and by the unusually high and varying receiver noise level of local origin.

Despite these severe limitations, we have been able to show that azimuths, zenith angles, and heights of reflection points can be explained satisfactorily by a source distribution for sporadic meteors which consists of an extended source centred on the apex of the Earth's way, together with more concentrated sources located on the ecliptic near the Sun and antisun. The direction and height data, together with the diurnal variation in the echo rate, require that the integrated strengths of the three sources be approximately the same.

Of particular interest is our conclusion that large increases in the sporadic echo rate observed during the summer months could be caused by abnormal ionospheric conditions. Should this be the case, it is not impossible that ionospheric conditions in the auroral zone could also influence the diurnal echo rate variation in some regular way.

VIII. Acknowledgments

The authors are indebted to Professor L. G. H. Huxley, who initiated the project, together with the Australian National Antarctic Research Expedition, under Mr. P. G. Law, who provided the facilities and finance for the experiment. The Radio Research Board also provided finance to build and maintain the equipment. The design and construction of the equipment were undertaken by Dr. W. G. Elford and Mr. E. L. Murray, and the authors also wish to thank Messrs. E. Burnett, I. Bird, and G. Cresswell for operating the equipment during 1958 and 1960. Miss J. Allister assisted in the reduction of the data.

One of us (C.S.N.) is a research student at the University of Adelaide and this paper was written whilst in receipt of a General Motors-Holden's Pty. Ltd. Post-Graduate Research Fellowship.

IX. References

Hawkins, G. S. (1956).—*Mon. Not. R. Astr. Soc.* **116** : 92.

Hawkins, G. S., and Prentice, J. P. M. (1957).—*Astr. J.* **62** : 234.

Kaiser, T. R. (1953).—*Advanc. Phys.* **2** : 495.

LOVELL, A. C. B. (1954).—" Meteor Astronomy." (Clarendon Press : Oxford.)
MCNAMARA, A. G. (1961).—*Canad. J. Phys.* **39** : 625.
MEEK, M. L., and JAMES, J. C. (1959).—*J. Atmos. Terr. Phys.* **16** : 228.
ROBERTSON, D. S., LIDDY, D. T., and ELFORD, W. G. (1953).—*J. Atmos. Terr. Phys.* **4** : 225.
WEISS, A. A. (1957).—*Aust. J. Phys.* **10** : 77.
WEISS, A. A. (1959).—*Aust. J. Phys.* **12** : 116.
WEISS, A. A. (1960*a*).—*Mon. Not. R. Astr. Soc.* **120** : 387.
WEISS, A. A. (1960*b*).—*Mon. Not. R. Astr. Soc.* **121** : 5.

APPENDIX

The Derivation of the Echo Rate as a Function of the Zenith Angle of a Source

The notation used in the paper is as follows :

χ is the zenith angle of a point radiant,
z is the zenith angle of a reflection point,
Z is the zenith angle of the centre of a source of radiants,
$\overline{\omega}$ is the minimum detectable power at the receiver,
α_0 is the limiting line density, i.e. the line density of a barely detectable echo,
P is the peak pulse power of the transmitter,
G_R, G_T are the gains of the receiving and transmitting antennas, respectively, over an isotropic radiator,
λ is the wavelength of the transmitted signal,
R is the range of the echo.

From Lovell (1954) we have :

$$\overline{\omega}=\frac{\alpha_0^2 PG_RG_T\lambda^3}{32\pi^2R^3}\cdot(e^2/mc^2)^2 \text{ for Lovell-Clegg scattering,} \tag{3}$$

and

$$\overline{\omega}=\alpha_0^{\frac{1}{2}}\frac{PG_RG_T\lambda^3}{54\pi^3R^3}\cdot(e^2/mc^2)^{\frac{1}{2}} \text{ for persistent scattering.} \tag{4}$$

For the Mawson equipment, $(G_RG_T)_{\text{max.}}=43$.

The above two formulae give rise to the same $\overline{\omega}$ at $\alpha_0=1\cdot17\times10^{12}$ electrons/cm, assuming that the transmitting and receiving antennas are normal $\frac{1}{2}\lambda$ dipoles. From (3) and (4) a table of α_0 as a function of G_RG_T, and hence of the zenith angle and azimuth of the reflection point, can be prepared. This table is not reproduced here.

We now wish to find the variation of echo rate, $F(Z)$, with source zenith angle Z, for any source for which the radiant density is a function only of ε, the elongation of the apparent radiant from the source. Referring to Figure 13, if A is the azimuth of arc ε from arc Z, we have $\cos\chi=\cos Z\cos\varepsilon+\sin Z\sin\varepsilon\cos A$, a standard formula of spherical trigonometry.

We must evaluate the integral

$$F(Z)=\int_{\varepsilon=0}^{\pi}\mathrm{d}\varepsilon\int_{A=0}^{2\pi}\mathrm{d}Af(\chi)D(\varepsilon)\sin\varepsilon, \tag{5}$$

where $D(\varepsilon)$ is the density distribution function of any source such that $D(\varepsilon)$ is independent of A. In practice, the limits of integration are determined by $f(\chi)$ becoming zero for a radiant below the horizon, i.e. for $\chi \geqslant 90°$, see Figure 8 (*a*). The integration is performed as follows: For given Z (at 10° intervals) and ε (at 5° intervals), compute $\chi(A)$ at 10° intervals of azimuth A. $\chi(A)$ is then replaced by the equipment response function, $f(\chi)$, discussed in Section V. Now integrate the tables of $f(\chi)$ with respect to angle A. This is the contribution

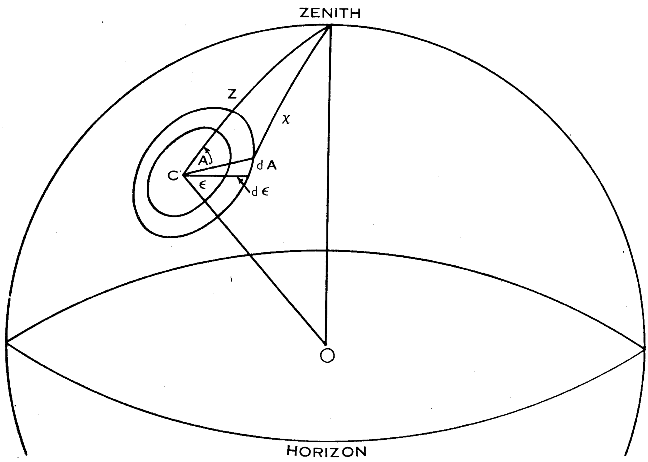

Fig. 13.—The geometry for the computation required to obtain the rate variation function $F(Z)$ from the equipment response function $f(\chi)$; for a source whose density is dependent only on the elongation ε from the source centre C. A is the azimuth variable for the integration, Z the zenith angle of the source centre, and χ the zenith angle of the element of radiant area.

of each annulus of given ε (Fig. 13) to the total rate. The area of each annulus of width $\mathrm{d}\varepsilon$ is $2\pi\sin\varepsilon\,\mathrm{d}\varepsilon$, hence the contributions of each annulus must be multiplied by $D(\varepsilon)\sin\varepsilon$ before summing over ε; we then have the echo rate as a function only of Z, i.e. $F(Z)$.

We shall now briefly discuss the density distribution functions $D(\varepsilon)$ used in these calculations. For the apex source, $D(\varepsilon)$ is an empirical function designed to fit the radio results of Weiss; it approximates an isotropic heliocentric distribution of meteors of velocity 50 km/sec. This velocity is hyperbolic and undoubtedly much higher than the true average velocity of sporadic meteors. This indicates that the distribution of radiants is not isotropic, and that the majority of orbits are in fact direct. $D(\varepsilon)$ for the apex source is plotted in Figure 14, together with the density function for the Sun and antisun sources.

The density distribution function for the Sun and antisun sources was chosen from a compromise of Weiss's radio data and an approximation to the visual data of Hawkins and Prentice. Once again, we have assumed radial symmetry about the centre. The radio distribution is a little broader than the

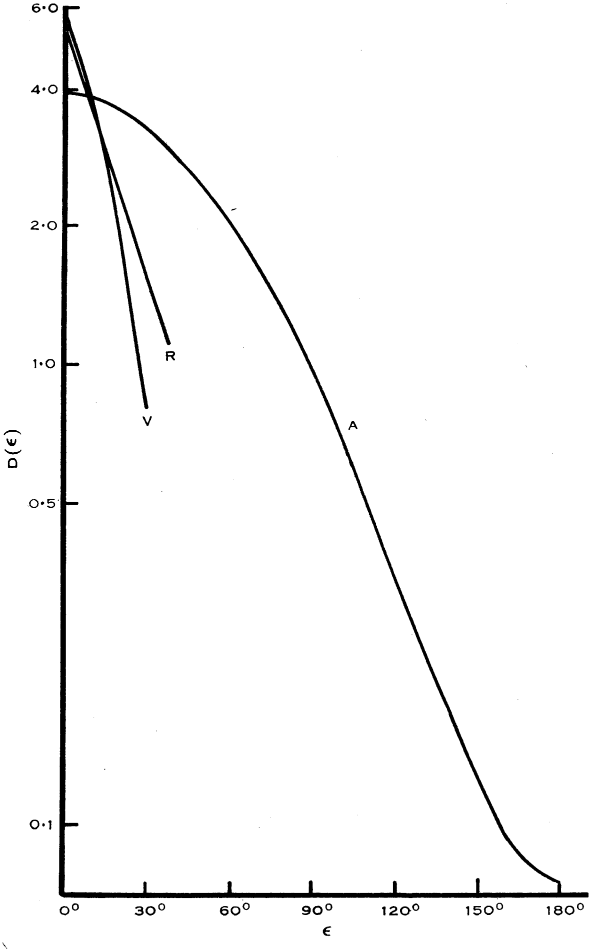

Fig. 14.—The density distribution function $D(\varepsilon)$ plotted against the elongation ε from the centre of the source. *A*, apex source; *R*, Sun and antisun sources, based on radio results; *V*, the antisun source, based on visual results.

visual distribution, but the difference is not significant. The peak density of radiants per square degree of sky for the antisun source was given by Hawkins and Prentice to be 1·5 times that of the apex and is shown as such in Figure 14. The value of this ratio has been discussed in Section V.